XXV. INTERACTION OF LASER RADIATION WITH PLASMAS AND NONADIABATIC MOTION OF PARTICLES IN MAGNETIC FIELDS[*]

Academic and Research Staff

Prof. T. H. Dupree
Prof. L. M. Lidsky
Prof. N. L. Oleson

Graduate Students

J. D. Callen
M. A. LeComte

P. Margosian
M. Murakami

A. A. Offenberger
L. C. Pittenger

RESEARCH OBJECTIVES AND SUMMARY OF RESEARCH

1. Nonadiabatic Scattering

The first stages in our study of nonadiabatic scattering have been completed. We have measured the lifetime of electrons subject to resonant perturbations in mirror and toroidal geometry. We have predicted the point at which first-order perturbation-theoretic estimates of velocity space diffusion fail and developed a new theory that is valid past this limit. We are now extending our experimental studies to very weak and to nearly resonant interactions. This should provide a sensitive test of certain facets of nonlinear plasma kinetic theory. We shall apply an earlier result to estimate the importance of nonlinear effects on the growth of ionospheric "whistlers."

M. Murakami, P. Margosian, L. M. Lidsky, D. J. Rose

2. Interaction of Coherent Radiation and Plasmas

With the modulated 80-W cw nitrogen-carbon dioxide laser and the (approximately) 10^{-13} W $(Hz)^{-1/2}$ bandwidth detector completed, we shall continue experiments on coherent scattering of 10.6-μ radiation from a steady-state plasma with electron density $\approx 10^{13}$ cm^{-3}, electron temperature ≈ 3-10 eV, 50-90% ionized. Our preliminary experiments have been troubled by very small signal-to-noise ratios, along with some nonplasma scattered laser light that is being detected. It appears that these problems can be reduced by simultaneously modulating the plasma and the laser and detecting the scattered signal at the difference frequency, and by using a narrow bandpass 10.6-μ filter cooled to $4.2\,°K$.

A. A. Offenberger, L. M. Lidsky, D. J. Rose

3. Laser-Plasma Science and Technology

This heading includes gaseous electronics, plasma physics, and technological aspects of devices that are likely to be of interest as gas lasers. This work continues with changes of detailed topics. We have completed design and testing of a particularly simple high-power argon ion laser. We are investigating properties of the

10. 6-μ N_2-CO_2-He laser system and relating them to the gaseous electronics of the laser discharge column. A pulsed N_2-CO_2 laser has been built and will be used to study pulse power peaking in the afterglow.

A. A. Offenberger, M. LeComte, L. M. Lidsky, D. J. Rose

A. INCOHERENT SCATTERING OF LIGHT FROM A PLASMA V

1. Laser-Plasma Scattering Experiment

The construction of an experiment for observation of 10. 6-μ laser scattering from a cw low-density plasma has been described previously.[1-3] Subsequently, two modifications have been made: (i) the detector, originally 10^{-3} cm^2, has been enlarged by nearly an order of magnitude to ease optical alignment problems; (ii) the plasma is being modulated in order that the remaining background scattered laser light can be discriminated against. The 10. 6-μ scattering modulated at frequency f_1, from a plasma modulated at f_2, will allow detection at $f_1 \pm f_2$, and discrimination from either f_1 or f_2. The primary beam dump consisting of a carbon-black inclined plane, plus baffles occluding a direct view of the input aperture to the plasma vacuum chamber by the detection optics, affords an isolation of 10^{-13}. The double modulation should easily increase isolation to view scattering levels of 10^{-14}.

The narrow-band optical filter (0. 14 μ) for detector S/N improvement, which was delivered in February 1967, proved defective and has been returned for recoating. The bandpass shifted by ~0. 3 μ, and consequently rejected the scattering for which we were looking at 10. 6 μ. This filter, which is essential for observing scattering through an improved S/N, has proved elusive and accounts for a one-year delay in concluding this experiment.

2. N_2-He Role in CO_2 Laser Excitation

A study of the role of He and N_2 in influencing CO_2 excitation in the CO_2 laser has yielded useful results, which are being prepared for publication. To summarize briefly, N_2 has a sharply peaked vibrational excitation cross section for electrons at 2.3 eV. For a Maxwellian electron energy distribution the resulting excitation is maximized for an electron temperature of ~1. 8 eV. Glow discharges in N_2 and CO_2 tend to produce electron distributions with a low T_e by virtue of the large number of low-energy molecular states degrading the electron energy gained from the applied electric field. Addition of large amounts of He tends to enhance T_e through electron-atom elastic collisions that convert electron drift energy to random thermal energy, without at the same time degrading energy via inelastic collisions (the minimum excitation energy of He being 19. 8 eV).

Experimental observation of He and/or N_2^+ line radiation as various gases were mixed in a discharge at constant current, enabled measurements of changes in T_e for various gas mixtures.

As expected, CO_2 in the discharge produced the lowest T_e, and the addition of He increased T_e to 1.7 eV, very near the calculated 1.8 eV at optimum lasing conditions. Simultaneous observation of the 4.3-μ spontaneous emission arising from the upper laser level (00°1) in CO_2 showed an increase of a factor of two on He addition, correlating the increase in upper-level population with increased T_e, as evidenced by enhanced N_2^+ line radiation. The detailed role of N_2 and the influence of He on CO_2 excitation are consequently better understood in the CO_2 laser.

3. CO_2 Modulation Experiment

We have current-modulated a 3-m CO_2 laser at both 120 cps and 840 cps with full-wave rectified 60 cycle from the wall, and 420 cycle from a motor generator. The resulting laser output is a fully modulated waveform of comparable average power to the DC excited laser, but with two additional features. The output power is essentially at one wavelength (> 90% at 10.59 μ) with greater stability than the DC laser, and, furthermore, has more power in lower T_{mn} modes. The last feature, of course, enables better focusing of the laser beam. The appearance of λ other than 10.59 μ occurs only at the beginning of each current cycle, and as the 10.59-μ transition saturates, the other lines disappear.

The modulated waveform shows features of the excitation and relaxation mechanisms, the details of which are being explored in a second paper that is being prepared for publication. Briefly, an He-CO_2 discharge shows a delay between current and lasing which decreases (from $\gtrsim 300$ μsec to ~50 μsec) with increasing He partial pressure; this delay is a direct measure of the lower laser state lifetime. The addition of N_2 smooths out the waveform (of delay, plus sharp leading pulse edge in the He-CO_2 discharge), thereby eliminating the initial pulse, and increases the laser cycle width to the current cycle width. This is consistent with the N_2 excitation role, whereby more readily excited N_2 molecules collisionally transfer their vibrational quanta to CO_2 in a continuous fashion. Moreover, the rate of N_2 transferring its excitation to CO_2, as inferred by Morgan and Schiff[4] can be shown to be incorrect. Their measurements gave a rate constant of 4.56×10^9 cm^3 $mole^{-1}$ sec^{-1}, or equivalently 249 sec^{-1} $Torr^{-1}$. Hocker et al.[5] have measured the upper laser state (00°1) collisional quenching and obtained 385 sec^{-1} $Torr^{-1}$, in which case the transfer rate, if true, would be largely collisionally deactivated. At our modulation period of 1.2 msec, we observe an order of magnitude increase in optical power with added N_2. Consequently, a more reasonable N_2-CO_2 transfer rate is 3850 sec^{-1} $Torr^{-1}$, since stimulated emission depopulates the upper laser level on a time scale that is

much faster than collisional destruction. The corresponding N_2-CO_2 transfer cross section at $20\,^{\circ}C$ is 1.9×10^{-18} cm^2.

A. A. Offenberger

References

1. A. A. Offenberger, Quarterly Progress Report No. 79, Research Laboratory of Electronics, M. I. T., October 15, 1965, pp. 145-147.

2. A. A. Offenberger, Quarterly Progress Report No. 81, Research Laboratory of Electronics, M. I. T., April 15, 1966, pp. 139-141.

3. A. A. Offenberger, Quarterly Progress Report No. 85, Research Laboratory of Electronics, M. I. T., April 15, 1967, pp. 223-225.

4. J. E. Morgan and H. I. Schiff, Can. J. Chem. 41, 903 (1963).

5. L. O. Hocker et al., Phys. Rev. Letters 17, 233 (1966).

B. VELOCITY SCATTERING OF CHARGED PARTICLES IN PERTURBED MAGNETIC FIELDS

In quasi-linear theory, particles whose velocity is equal to a wave's phase velocity can resonate with the wave and thereby increase their kinetic energy (or diffuse in velocity space). The rate of the increase is balanced by the rate of decrease of wave energy which yields the well-known Landau damping in the longitudinal case. Once the resonant particle is trapped in the wave, however, strong wave-particle interaction occurs, the linear damping theory is no longer valid.[1] Dupree has presented a new perturbation theory based upon use of a statistical ensemble of the exact particle orbits, instead of the unperturbed orbits.[2] Therefore particle-orbit consideration becomes more important; however, in the existence of an external magnetic field, particle-orbit calculation is not a simple matter.

Regarding nonadiabatic injection of charged particles into thermonuclear devices, Wingerson proposed[3] the "corkscrew," using an external magnetic field helical perturbation in such a way that the designed particle resonates with the perturbation field so that the particle is accelerated perpendicularly to the main confining field. The already trapped particles resonate with the perturbation field, however, and lose their perpendicular energy and escape from the confining region. Therefore the scattering process in velocity space, because of the perturbation field, is important for estimating the loss rate. Clarke performed corkscrew experiments in magnetic-mirror geometry[4,5] and Moir in toroidal geometry.[6,7] These experiments and Clarke's numerical experiment[5,8] show that the unperturbed orbit theory does not hold when the magnetic field perturbation becomes great.

We are constructing an experimental device to investigate the velocity scattering of

charged particles in perturbed magnetic fields. We shall use electrostatically trapped electrons as proposed by Moir.[7] We shall describe the experimental arrangement and development of a fast-rising high-voltage square pulser. Some simple theory will be described, which explains qualitatively some of Clarke's numerical results and the analogy of this work to electrostatic waves in terms of "trapped" and "untrapped" particles in the perturbation field.

1. Experiment

Figure XXV-1 shows the experimental arrangement. A uniform axial magnetic field is produced by 30 water-cooled, 24 in. I.D. solenoids. The operation field strength is 100 Gauss, which gives a Larmor radius of 1.3 cm for a totally wound-up electron
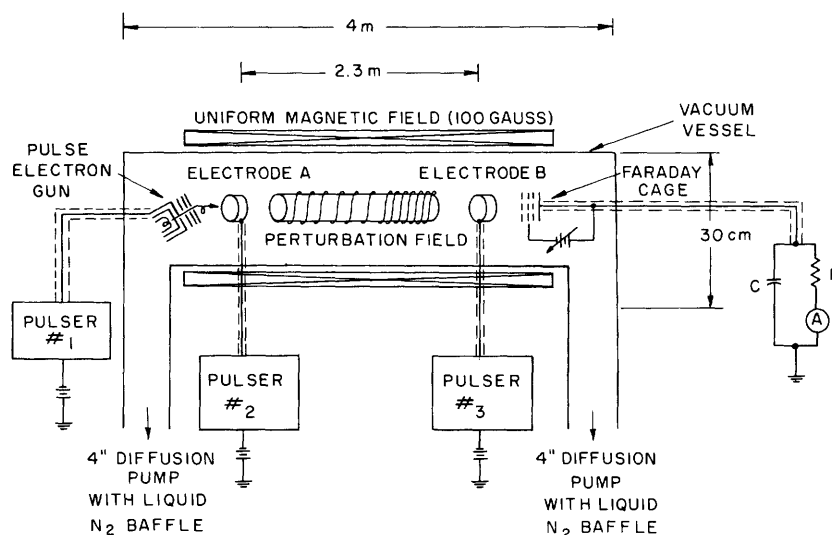

Fig. XXV-1. Experimental arrangement.

with energy of 1600 eV. The perturbation field winding is placed inside the vacuum vessel. Two axially trapping electrodes are spaced at a distance of 2.3 m, which corresponds to a transit time of 100 nsec for the electrons moving parallel to the axis with 1600-eV energy. A pulsed electron gun is located near one end of the main field, and produces electron beam pulses of 1600-eV energy. A Faraday cage with retarding potential grids is placed at the other end.

Figure XXV-2 illustrates the pulsing scheme. While the two electrodes are usually biased at −1800 V, pulser No. 2 supplies a +1800 V positive pulse so that no potential barrier exists. In this situation, the pulsed electron gun injects a 1600-eV electron beam. The electrons penetrating into the trapping region are reflected at trapping electrode B. Before the electrons return to electrode A, the applied positive pulse on
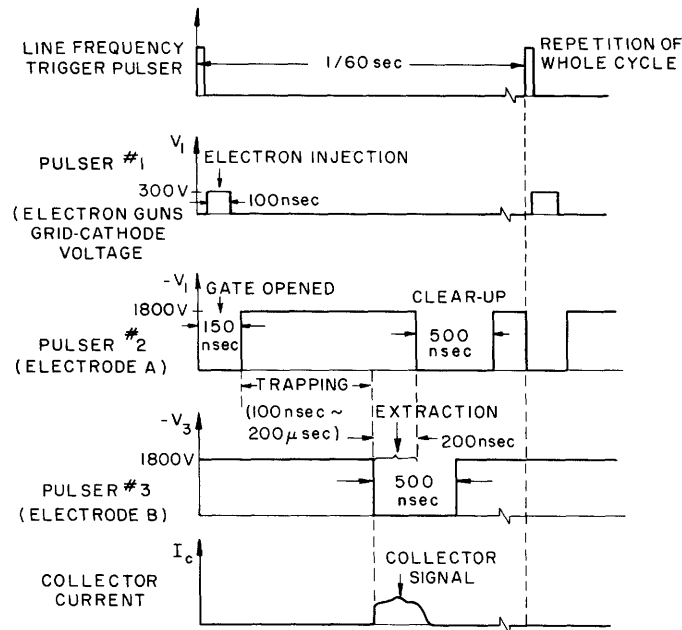
Fig. XXV-2. Pulse scheme.

electrode A is turned off, so that the electrons cannot escape from the region. The electron beam has been gated off before the pulse so electrode A is shut off. Now the electrons are trapped between both electrodes, and interact with the perturbation field, which leads the electron velocity distribution to change from a δ-function to a broader one. After some trapping time, which is variable from 100 nsec (1 one-way transit) to 200 μsec (1000 two-way transits), a positive pulse is applied to electrode B in order to extract the electrons from the interaction region to the detector, which is composed of a Faraday cage with a variable retarding potential grid. To clear up the electrons that have been rejected at the retarding grid, a positive pulse is applied to electrode A so that those electrons are damped at the vacuum wall.

In the existence of both magnetic field and electric field, particles drift by velocity $\underline{E} \times \underline{B}/B^2$, which is perpendicular to $\underline{B}$ and independent of the particle velocity. Since the desired velocity distribution is taken from the differentiation of collector currents with respect to the retarding potential, the shape of the velocity distribution is not affected by $\underline{E} \times \underline{B}$ drift, but it does shift the whole distribution. Therefore we require $\underline{E} \times \underline{B}$ drift, and, hence, that E_r be as small as possible. We have examined electric field uniformity for several electrode geometries in an electrolytic tank, and it appears that toroidal trapping electrodes are preferable to grids or simple cylinders.

A pulsed electron gun has been designed and is under construction. The wide modulation bandwidth (up to a few GHz) requires a coaxial structure of cathode and control grid.

High vacuum is necessary so that the trapped electrons will not change their velocity as a result of collisions with residual gases. Although we utilize O-ring gaskets, our preliminary vacuum test shows that it is possible to get at least a few times 10^{-8} Torr, if we have the system up to 120 °C and use liquid-nitrogen cold traps.

As we have said, we need several fast-rising fast-falling high-voltage square pulsers. If the pulse rises slowly, then a larger portion of the electrons is accelerated by the transient electric field, and the velocity distribution is changed. Therefore
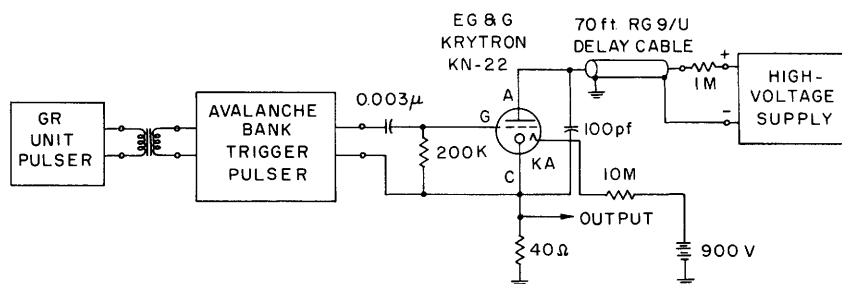

Fig. XXV-3. Square-pulse generator.

we require a square pulser whose pulse height is 1800 V, duration is 200 nsec, and rise and fall times are less than 5 nsec. The circuitry is shown in Fig. XXV-3.

The avalanche bank trigger pulser (see Fig. XXV-4) is composed of 8 transistors in series, operated in the avalanche mode. In the quiescent state the high-voltage DC power supply charges the two capacitors up to 1100 V, which is resistor-divided into eight 135-V segments, each of which is applied to a single transistor. A trigger pulse triggers the avalanche breadown of the series of transistors; this discharges the capacitors through the load resistor R_L. In this circuitry we can get a 900-V pulse with 3-nsec rise time. After the discharge, which is determined by time constant CR_L, the transistors return to their quiescent state, and again charges are accumulated on the capacitor C with time constant CR_C.
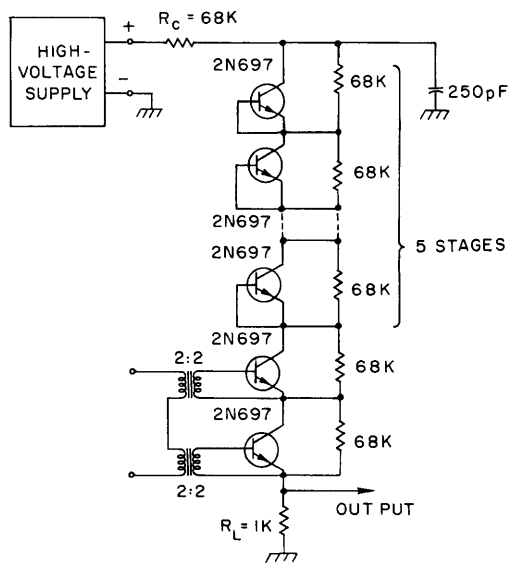
In the main circuitry we use an EG and G-type KN-22 cold-cathode trigger tube. In the quiescent state the delay cable stores the charge at 3000 V. When, in response to a

Fig. XXV-4. Avalanche bank trigger-pulse circuit.

trigger pulse of the avalanche bank, the krytron breaks down, a negative voltage step is applied to the line. When this voltage wave reaches the end of the line, it is reflected as a positive voltage step, because of the open circuit. At the time of the two-way transit, the positive voltage step reaches the beginning of the line. If the resistance across the line is equal to or less than the characteristic impedance, no reflection or negative voltage reflection occurs. Therefore the discharge in the kryton cannot be sustained any more and quenches. We use a 40-Ω load which gives no further reflection on the tail of the output. (We have tried a 50-Ω load, which has been found to give further reflection.) The capacitor C between the anode and the cathode, which has been empirically optimized at 100 pF, acts to stabilize the discharge at the rising part and to by-pass the high-frequency components to help the discharge quench quickly.

Figure XXV-5 shows a total voltage pulse across the load resistor R_L when the delay line was charged to 3 kV. The pulse height is 1550 V and the pulse duration is 220 nsec, which is the two-way transit time of the cable. In the measurements
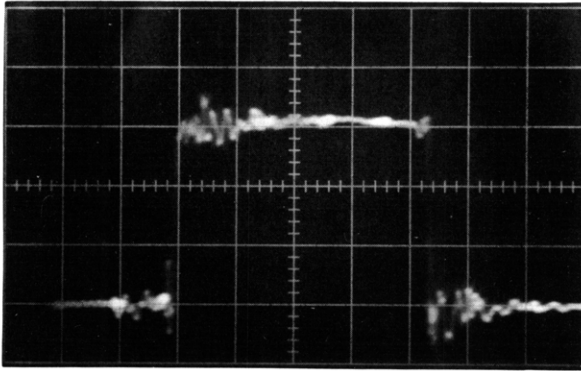

Fig. XXV-5. Output signal of the square-pulse generator.
Vertical: 500 V/div.
Horizontal: 50 nsec/div.

with the Tektronix Type 454 oscilloscope (rise time, 2.5 nsec), the 10-90% rise time of the pulse is 3.5 nsec, and the 90-10% fall time is 4 nsec. Thus far, we have not been able to get rid of the oscillations on the front of the pulse.

2. Theory

Newton's equation for the motion of a particle in a magnetic field is

$$\frac{d\underline{v}}{dt} = \frac{q}{m} \underline{v} \times \underline{B}. \tag{1}$$

Our magnetic field $\underline{B}$ is composed of a uniform axial magnetic field $\underline{B} = B_o \hat{\underline{e}}_{\parallel}$ and a small perturbation magnetic field $\underline{B}_{\perp} = \beta B_o \hat{\underline{e}}_{\perp}$, that is,

$$\underline{B} = B_o (\hat{\underline{e}}_{\parallel} + \beta \hat{\underline{e}}_{\perp}). \tag{2}$$

If β is small, dominant perpendicular motion is gyration about the main axial field lines; therefore, for the particle near the axis, $v_\perp \approx v_\theta$. Using this approximation with the energy conservation $\left(v_o = v_\parallel^2 + v^2\right)$, we can reduce Eq. 1 to a simpler equation[9]

$$\frac{dv_\perp}{dz} = \omega_\perp \cos \chi,$$ (3)

where $\omega_\perp = qB_\perp/m$.

If we define χ by the angles between the direction of the particle's perpendicular velocity and that of the perturbation magnetic field, then change in angle χ with respect to distance z is the reciprocal of particle orbit pitch minus the reciprocal of the perturbation field pitch P, that is

$$\frac{d\chi}{dz} = \frac{\omega_o}{u_\parallel} - \frac{2\pi}{P},$$ (4)

where $\omega_o = qB_o/m$. (The validity of the approximation $v_\perp \approx v_\theta$ was checked by numerically comparing the orbits of (1) and (4) with those of (3) and (4), and it turned out that the approximation is valid when $v_\perp^2/v_o^2 \gtrsim 0.25$.) Let us use the normalized values $u_\perp = v_\perp/v_o$, $u_\parallel = v_\parallel/v_o$, $\zeta = zr_o$, $p = P/r_o$, where $r_o = v_o/\omega_o$ is the Larmor radius of the totally wound up particle (that is, $v_\perp = v_o$). Then

$$\frac{du_\perp}{d\zeta} = \beta(\zeta) \cos \chi$$ (5)

$$\frac{d\chi}{d\zeta} = \frac{1}{u_\parallel} - \frac{2\pi}{p(\zeta)}.$$ (6)

In the corkscrew, $p(\zeta)$ is specially arranged in such a way that a chosen particle can resonate (that is, $d\chi/d\zeta = 0$) with the externally applied perturbation field, and also $\beta(\zeta)$ is sinusoidally changed to avoid nonadiabatic effects at the end of the perturbation field.

Let us consider the case of a perturbation field with a constant pitch ($p(\zeta) = $ constant) and a constant amplitude ($\beta(\zeta) = $ constant). We expand the term $1/u_\parallel$ in terms of the variation $\Delta u_\perp$

$$\frac{1}{u_\parallel} = \frac{1}{\sqrt{1 - u_\perp^2}} \cong \frac{1}{u_{\parallel o}}\left\{1 + \frac{u_{\perp o}}{u_{\parallel o}^2} \Delta u_\perp\right\},$$ (7)

where the values with the suffix o are those at $\zeta = 0$. Then

$$\frac{d\Delta u_\perp}{d\zeta} = \beta \cos \chi$$ (8)

$$\frac{d\chi}{d\zeta} = \gamma + A\Delta u_\perp,$$ (9)

where

$$\gamma = \frac{1}{u_{\|0}} - \frac{2\pi}{p}$$ (10)

$$A = \frac{u_{\perp 0}}{u_{\|0}^3}.$$ (11)

The combination of (8) and (9) gives us

$$\frac{d^2\chi}{d\zeta^2} = A\beta \cos \chi.$$ (12)

Notice its similarity to an equation governing the motion of a pendulum under gravity without any damping (in this case ζ stands for time). The energy integral of Eq. 12 yields the relation

$$\left(\frac{d\chi}{d\zeta}\right)^2 - 2A\beta \sin \chi = K(\text{constant})$$ (13)

which is plotted in various K in Fig. XXV-6.

For a pendulum, $d\chi/d\zeta$ is considered to be angular velocity. When the constant K is small, the pendulum oscillates around the equilibrium position. If the constant K
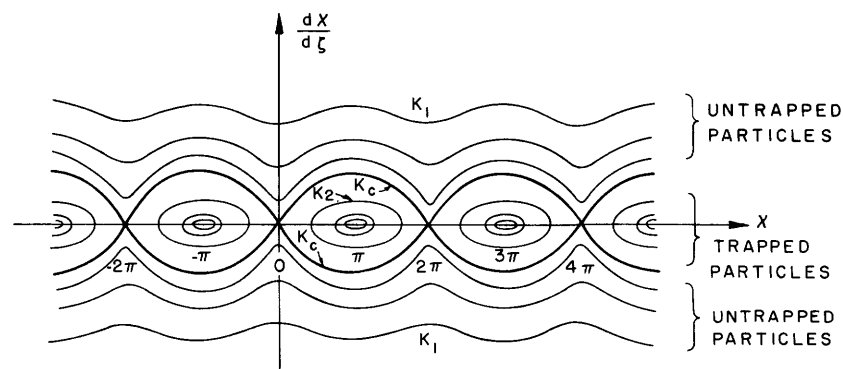

Fig. XXV-6. Phase plot of the integral.

becomes larger than K_c (which corresponds to the separatrix shown in bold lines), the motion becomes rotary and the angular velocity $d\chi/d\zeta$ is oscillatory. The same situation appears in O'Neil's calculation,[1] in which he solved the Vlasov equation exactly for

the resonant electron.

It is adequate to call a particle with K_1 a "trapped" particle, and to call a particle with K_2 an "untrapped" particle, where $K_1 > K_c > K_2$. (The terminology "trapping" is also used in the experimental part, but it is obviously different here.)

Let us consider the integral constant, K. Since at $\zeta = 0$ $\Delta u_\perp = 0$, and $d\chi/d\zeta = \gamma$, from Eq. 13,

$$K = \gamma^2 - 2A\beta \sin \chi_0. \tag{14}$$

Now let us assume that γ is not small. This means that the particle is "nonresonant" to the perturbation. For a corkscrew, it is applicable to dissociated particles, and also to particles whose magnetic moment is large so that the resonant position is near the end of the corkscrew where the magnitude is small. If β is small, then the term $2A\beta \sin \chi_0$ in Eq. 14 is not significant, and K is large and independent of the initial angle χ_0. Therefore particles with any initial angle stay on one curve in the untrapping range. These particles "go over the hill and dale" in χ. From Eq. 8, we can see that Δu is oscillatory, too. Therefore we can expect that $\langle \Delta u_\perp \rangle \cong 0$ and $\langle \Delta u_\perp^2 \rangle \neq 0$ generally, which will be proved. If we have a randomization such as the phase-mixing mirrors in our experimental system, then the scattering process is diffusive, and the diffusion coefficient is proportional to $\langle \Delta u_\perp^2 \rangle$. We shall show that a simple perturbation technique works for this case, and that it agrees with the exact solution.

If γ^2 becomes comparable with $2A\beta$ (that happens for resonant particles or large-amplitude perturbation), K becomes small and also dependent on the initial angle χ_0. Therefore even for the group of particles whose initial perpendicular velocity $u_{\perp o}$ is the same, some might be trapped, and some untrapped. Therefore the resultant change $\Delta u_\perp$ does depend on the initial angle χ_0. This explains qualitatively the strong dependence of $\langle \Delta u_\perp \rangle$ on χ_0 in Clarke's[4,5] and our preliminary numerical calculations for the corkscrew. In this situation, the process of the scattering is no longer diffusive.

Since the change in $\Delta u_\perp$ for those particles is secular, simple perturbation techniques do not work. Note that since, in deriving Eq. 9, we have used the approximation Eq. 7, we cannot go farther in the discussion of the trapped particles, except for some physical intuition. Clarke used the stationary phase method in the evaluation of the integral for $\Delta u_\perp$.[5] This is justified because the contribution of $\Delta u_\perp$ comes from the portion in which the particle is trapped, and in the rest of the portion the particle is untrapped and gives less contribution.

The transition from untrapped to trapped particles is given by the criterion

$$\gamma^2 = 2A\beta_c \tag{15}$$

or

$$\beta_c = \frac{\gamma^2}{2A} = \frac{u_{\parallel o}}{2u_{\perp o}} \left(1 - \frac{u_{\parallel o}}{u_p} \right)^2 , \tag{16}$$

where $u_p = p/2\pi$. Therefore any small perturbation can cause trapping if a perturbation pitch resonates with a particle pitch. The trapping is characteristically nonlinear, and there is no linear counterpart, although the untrapped particle cases reduce to the usual helices of zero-order theory as the perturbation amplitude tends to zero.[10]

Let us use simple perturbation technique to solve the equation for a nonresonant particle. χ is expanded in terms of the small parameter β, that is,

$$\chi = \chi^{(o)} + \beta \chi^{(1)} + \beta^2 \chi^{(2)} + \dots . \tag{17}$$

Substituting this in Eq. 12, we separate the terms of zeroth and first order in β:

$$\frac{d^2\chi}{d\zeta^2} = 0 \tag{18}$$

$$\frac{d^2\chi}{d\zeta^2} = A \cos \chi^{(o)}. \tag{19}$$

From Eq. 11,

$$\chi^{(o)} = \gamma\zeta + \chi_o. \tag{20}$$

Then Eq. 12 with Eq. 13 gives

$$\chi^{(1)} = -\frac{A}{\zeta^2} \cos (\gamma\zeta + \chi_o) + c\zeta + d. \tag{21}$$

If we claim the integral, Eq. 12, holds to the order of β, the secular term $c\zeta$ vanishes, and we get

$$\chi = \gamma\zeta + \chi_o - \frac{A\beta}{\gamma^2} \cos (\gamma\zeta + \chi_o) + o(\beta^2). \tag{22}$$

Substituting this in Eq. 7 with initial condition $\Delta u = 0$ at $\zeta = 0$, we get

$$\Delta u_\perp = -\frac{\beta}{\gamma} \left[\sin (\gamma\zeta + \chi_o) - \sin \chi_o - \frac{A\beta}{\gamma^2} \{ \cos (\gamma\zeta + \chi_o) - \cos \chi_o \} \right]. \tag{23}$$

The first and second coefficients of the Fokker-Planck equation describing the evolution of the distribution in the velocity space are

$$\left\langle \Delta u_\perp \right\rangle \equiv \frac{1}{2\pi} \int_0^{2\pi} (\Delta u_\perp) \, d\chi_0 = o(\beta^3) \tag{24}$$

$$\left\langle \Delta u_\perp^2 \right\rangle \equiv \frac{1}{2\pi} \int_0^{2\pi} (\Delta u_\perp)^2 \, d\chi_0 = \frac{\beta^2}{\gamma^2} (1 - \cos \gamma\zeta) + o(\beta^4) \tag{25}$$

Now let us use the integral Eq. 10 to derive the exact solution for the untrapped particles.

$$\frac{d\chi}{d\zeta} = \frac{2\sqrt{A\beta}}{\kappa} [1 - \kappa^2 \sin^2 \eta]^{1/2}, \tag{26}$$

where

$$\eta = \frac{\chi}{2} + \frac{3}{4}\pi \tag{27}$$

$$\kappa^2 = \frac{4A\beta}{K - 2A\beta} = \frac{4A\beta}{\gamma^2 - 2A\beta \sin \chi_0}. \tag{28}$$

Since we are treating the untrapped particle case, κ^2 is almost independent of χ_0 and $\kappa^2 = \frac{4A\beta}{\gamma^2} \ll 1$. The differential equation (26) is solved as

$$F(\eta, \kappa) - F(\eta_0, \kappa) = \frac{\sqrt{A\beta}}{\kappa} \zeta, \tag{29}$$

where $F(\eta, \kappa)$ is the elliptic integral of the first kind with parameter κ. Then from Eqs. 7 and 22, with the initial condition, we get

$$\Delta u_\perp = \frac{2}{\kappa}\sqrt{\frac{\beta}{A}} \left\{ dn[F(\eta_0, \kappa)] - dn\left[\frac{\sqrt{A\beta}}{\kappa} \zeta + F(\eta_0, \kappa) \right] \right\}$$

$$= \frac{2}{\kappa}\sqrt{\frac{\beta}{A}} \left\{ \sqrt{1 - \kappa^2 \sin^2 \eta_0} \right.$$

$$\left. - \frac{\sqrt{1 - \kappa^2 \sin^2 \eta_0} \, dn\left(\frac{\sqrt{A\beta}}{\kappa} \zeta\right) - \kappa^2 \sin\eta_0 \cos\eta_0 \, sn\left(\frac{\sqrt{A\beta}}{\kappa} \zeta\right) cn\left(\frac{\sqrt{A\beta}}{\kappa} \zeta\right)}{1 - \kappa^2 \sin^2 \eta_0 \, sn^2\left(\frac{\sqrt{A\beta}}{\kappa} \zeta\right)} \right\}. \tag{30}$$

Now we average $\Delta u_\perp$ and $\Delta u_\perp^2$ over the initial angle η_0. Although it is possible to express the averaged values in terms of Jacobian elliptic integrals and other elliptic integrals,

some of them have no simple power representations for small κ. Therefore, we expand $\sqrt{1 - \kappa^2 \sin^2 \eta_0}$ in terms of κ before integrating them over η_0. Then the coefficients are

$$\left\langle \Delta u_\perp \right\rangle = o(\beta^3) \tag{31}$$

$$\left\langle \Delta u_\perp^2 \right\rangle = \frac{\beta^2}{\gamma^2} (1 - \cos \gamma \zeta) + o(\beta^4). \tag{32}$$

These agree with the results (Eqs.24 and 25) of the simple perturbation techniques.

M. Murakami, L. M. Lidsky

References

1. T. O'Neil, Phys. Fluids **8**, 2255 (1965).

2. T. H. Dupree, Phys. Fluids **9**, 1773 (1966).

3. R. C. Wingerson, Phys. Rev. Letters **6**, 446 (1961).

4. J. F. Clarke, Quarterly Progress Report No. 81, Research Laboratory of Electronics, M.I.T., April 15, 1966, pp. 147-159.

5. J. F. Clarke, Sc.D. Thesis, Department of Nuclear Engineering, M.I.T., 1966.

6. R. W. Moir and L. M. Lidsky, Quarterly Progress Report No. 85, Research Laboratory of Electronics, M.I.T., April 15, 1967, pp. 225-229.

7. R. W. Moir, Sc.D. Thesis, Department of Nuclear Engineering, M.I.T., 1967.

8. J. F. Clarke and L. M. Lidsky (unpublished).

9. R. G. Wingerson, T. H. Dupree, and D. J. Rose, Phys. Fluids **7**, 1475 (1964).

10. R. L. Lutomirski and R. N. Sudan, Phys. Rev. **147**, 156 (1966).